DOI 10.1007/s11029-022-10049-8
Mechanics of Composite Materials, Vol. 58, No. 4, September, 2022 (Russian Original Vol. 58, No. 4, July-August, 2022)

INVESTIGATING THE INSTABILITY OF PARAMETRIC VIBRATIONS OF COMPOSITE PLATES UNDER ARBITRARY PULSATING LOADS BASED ON HIGH-ORDER PLATE THEORIES

C. S. Chen,[1] H. Wang,[2] J. Y. Kao,[1] and W. R. Chen[3*]

Keywords: *excitation frequency, dynamic instability index, Mathieu-type motion, Bolotin's method*

The instability of composite plates subjected to an arbitrary periodic dynamic loading is investigated based on Lo's high-order shear-deformation plate theory. The differential equations of motion of Mathieu-type are formed by Hamilton's principle and employing the Galerkin method. Using Bolotin's method, the excitation frequencies of composite plates are evaluated to determine their dynamic stability region and dynamic instability index. Omitting the high-order terms of Lo's displacement field, the system equations can be simplified to governing equations in the first-order plate theory. The dynamic instability determined by the present theory is compared with results of the first-order plate theory. Results show that high order terms have a significant impact on the dynamic instability of composite plates.

1. Introduction

Since composite plates can provide a higher strength- and stiffness-to-weight ratios than the traditional metal plates, they are widely used in many engineering fields. The dynamic instability of the plates is a phenomenon that requires special attention in the design of structural components. The instability in the form of parametric resonance may occur when a such structure is subjected to a periodic dynamic loading. How to accurately determine the dynamic instability region of

[1]Department of Mechanical Engineering, Lunghwa University of Science and Technology, Guishan Shiang 33306, Taiwan
[2]Department of Mechanical Engineering, Ming Chi University of Technology, Tai-Shan 24301, Taiwan
[3]Department of Mechanical Engineering, Chinese Culture University, Taipei 11114, Taiwan
[*]Corresponding author; e-mail: wrchen@faculty.pccu.edu.tw

Russian translation published in Mekhanika Kompozitnykh Materialov, Vol. 58, No. 4, pp. 783-812, July-August, 2022. Russian DOI: 10.22364/mkm.58.4.08. Original article submitted February 2, 2021; revision submitted August 27, 2021.

the plates is a very important topic in practical applications. A comprehensive study of dynamic stability problems under periodical loadings has been performed by Bolotin [1]. Vijayaraghavan [2] studied the dynamic instability of cylindrical thin shells subjected to in-plane loads under sinusoidal base excitations. The linear bending theory used in this analysis is sufficient to predict the onset of their dynamic instability.

The dynamic resonance is one of the most important subjects in studying the dynamic instability characteristics of structures. Mohamad [3] presented a broad review on the studies of the dynamic behavior of composite shells. Fazilati [4] investigated the dynamic instability of composite laminated structures subjected to axially harmonic loadings using two types of finite-strip method. Results showed that the present model is capable of predicting the parametric resonance of the structures investigated. The parametric instability of composite curved panels under nonuniform axial loadings were also studied by Ovesy [5] based on the finite-strip method. The static and dynamic components of the load varied according to a parabolic function. Bolotin's method was used to investigate the effects of loading and geometric parameters on the instability regions. Kao [6] applied Bolotin's method to studying the dynamic instability of foam-filled sandwich plates under a periodic loading. The dynamic instability index was used to investigate the effects of various parameters affecting the dynamic stability behavior of the plate. Chen [7] investigated the dynamic instability of composite plates subjected to periodic loads based on the first-order theory. Bolotin's method was used to solve Mathieu–Hill differential equations to determine the dynamic instability region. Darabi [8] studied the nonlinear dynamic instability of composite plates under harmonic loadings. The nonlinear Mathieu–Hill equations were obtained based on the Galerkin method. Then, Bolotin's method was applied to determining the dynamic instability regions and unstable vibration amplitudes. The dynamic instability behavior of laminated composite sandwich plates was investigated by Sahoo [9] based on the zigzag theory, which takes into account the nonlinear distribution of transverse shear stresses. An efficient finite-element method was developed for studying the dynamic instability. The excitation frequency boundaries of principal instability regions were determined using Bolotin's method. The dynamic instability of composite plates with variable stiffness under periodic loads was studied by Rasool [10]. A set of Mathieu–Hill equations of motion was obtained by the modal transformation technique and was solved by a multiple scales method to determine the dynamic instability regions associated with various types of resonance. Mohanty [11] studied the dynamic instability of delaminated composite plates under periodic loads by the finite-element method based on the first-order shear deformation plate theory. Bolotin's method was also employed to evaluate the boundaries of instability zones. Results showed that the increasing delamination shifted the instability region lower excitation frequencies.

However, the classical and first-order plate theories cannot adequately model the behavior of composite structures. Therefore, various high-order plate theories have been proposed to improve their accuracy. Lee [12] analyzed the dynamic stability of laminated composite skew plates under periodic loads based on a high-order plate theory. The dynamic instability regimes were determined by Bolotin's method, and the influence of the pulsating load on the dynamic instability index was discussed. The dynamic instability of sandwich plates with carbon-nanotube-reinforced face sheets under periodic forces was studied by Sankar [13]. The effect of carbon nanotube volume fraction and core-surface layer thickness on the instability region and its excitation frequency was investigated. Based on first-order and high-order theories, Ramachandra [14] studied the dynamic instability of composite plates under uniform, linear, and parabolic dynamic loads. The dynamic instability regions were determined for various periodic loads using Bolotin's method. The influences of load types, aspect ratio, and restraint conditions were investigated. Noh [15] investigated the dynamic instability of delaminated composite skew plates subjected to periodic loads by using a high-order plate theory. The boundaries of the unstable regions were obtained by Bolotin's method. The effects of skew angle, fiber angle, delamination lengths, and static and dynamic load factors on the dynamic instability characteristics were discussed. The dynamic stability of composite skew plates under parabolic and linear periodic loads based on higher order plate theory was studied by Kumar [16]. Following Bolotin's method, the dynamic unstable regions were evaluated based on a high-order approximation method. The effects of various geometric parameters, loading types, and boundary conditions were investigated. Based on a polynomial high-order plate theory, Adhikari [17] examined the dynamic instability of composite plates under periodic loads with various nonuniform distributions. Mathieu-type equations were formulated and then solved using Bolotin's method to obtain the

dynamic instability regions. The influence of various kinds of nonuniform harmonic loading on the parametric instability behavior of the plates was studied.

The dynamic instability of composite plates has been investigated by many researchers, but studies on the dynamic instability of composite plates under arbitrary periodic loads with bending and normal stress by using a high-order plate theory are rare. Therefore, the present work is devoted to the dynamic vibration instability of composite plates subjected to an arbitrary periodic load based on a high-order Lo, Christensen and Wu [18] plate theory. Hamilton's principle is utilized to establish the governing partial differential equations of motion, which are then reduced to ordinary differential equations by using the Galerkin method. Employing Bolotin's method, a set of ordinary differential equations of Mathieu–Hill type is established and solved to obtain the excitation frequencies of composite plates. Their dynamic instability region and dynamic instability index are determined through the excitation frequencies to investigate the dynamic instability behavior of composite plates. The difference between the effects of high-order and first-order plate theories on the dynamic instability regions and indices is studied.

2. Basic Formulation

Let us establish the dynamic governing equation of a composite plate under the general state of time-varying external force using Hamilton's principle as described by Brunelle [19], to derive the governing equations of motion of the plate, namely,

$$\delta\int_{t_0}^{t_1}\left(U_S - K_t - W_i - W_e\right)dt = 0\,, \tag{1}$$

where $U_s = \int_{V_0}\sigma_{ij}\varepsilon_{ij}dV$, $K_t = \frac{1}{2}\int_{V_0}\rho\dot{v}_i\dot{v}_i dV$, $W_i = \int_{V_0}X_i v_i dV$, $W_e = \int_{S_0}p_i v_i dS$.

Here, δ is the variation of a function; U_S and K_t are potential and kinetic energies; W_i and W_e are internal and external works; σ_{ij} and ε_{ij} are the stress and strain fields; ρ and v_i are the mass density and displacements; X_i is the body force per unit initial volume; p_i is the surface force per unit area; V_0 and S_0 are the volume and the boundary surface. Inserting the integral forms of U_S , K_t, W_i , and W_e into Eq. (1), performing variational operations, and assuming that δv_i disappears at times t_0 and t_1, Eq. (1) becomes

$$\int_{t_0}^{t_1}\left[\int_{V_0}\left(\sigma_{ij}\delta\varepsilon_{ij} - X_i\delta v_i - \rho\ddot{v}\delta v_i\right)dV - \int_{S_0}\left(p_i\delta v_i\right)dS\right]\,dt = 0\,. \tag{2}$$

According to the Lo, Christensen and Wu theory, the incremental displacements $u, v,$ and w at any position assume the following forms:

$$u\left(x,y,z,t\right) = u_x\left(x,y,t\right) + z\varphi_x\left(x,y,t\right) + z^2\xi_x\left(x,y,t\right) + z^3\phi_x\left(x,y,t\right), \tag{3}$$

$$v\left(x,y,z,t\right) = u_y\left(x,y,t\right) + z\varphi_y\left(x,y,t\right) + z^2\xi_y\left(x,y,t\right) + z^3\phi_y\left(x,y,t\right), \tag{4}$$

$$w\left(x,y,z,t\right) = w\left(x,y,t\right) + z\varphi_z\left(x,y,t\right) + z^2\xi_z\left(x,y,t\right). \tag{5}$$

Equations (3)-(5) are obtained by expanding the displacements $u, v,$ and w into Taylor series in terms of the thickness variable z to take into account the parabolic variation of transverse shear strains and the nonlinear change of transverse normal strains across the plate thickness. Therefore, in the Lo, Christensen, and Wu theory, in-plane displacements are expanded into cubic functions of the thickness variable by Taylor series, and the lateral displacement is expanded as a square function. Eleven unknowns, including high-order flexural deformation modes, are considered in the displacement field. Concerning other displacement-based theories in this field, it is worth mentioning that the expansion of different power of the thickness coordinate results in different theories with various unknowns. The simplest is the first-order shear deforma-

tion theory with five unknowns [20, 21]. A high-order shear deformation theory with seven unknowns was presented by Essenburg [22], and another one with nine unknowns was developed by Pandya [23]. In addition, a third-order shear deformation theory with five unknowns was developed by Levinson [24] and Reddy [25] considering the requirement that the transverse shear stresses have to vanish at the top and bottom surfaces of the plate to reduce the displacement field of nine unknowns to that with five variables. Further, Lo's high-order transverse shear and normal deformations theory will be designated as NSNT. Ignoring higher order normal strains in Eqs. (3) and (4), and dropping the transverse shear strains in Eq. (5), the displacement field of the simple first-order shear deformation theory (FSDT) is obtained. The stress–strain relationship for a k th layer of a composite plate, made of a monoclinic material can be written as

$$\begin{bmatrix}\sigma_{xx}\\ \sigma_{yy}\\ \sigma_{zz}\\ \sigma_{yz}\\ \sigma_{zx}\\ \sigma_{xy}\end{bmatrix}=\begin{bmatrix}C_{11} & C_{12} & C_{13} & 0 & 0 & C_{16}\\ C_{12} & C_{22} & C_{23} & 0 & 0 & C_{26}\\ C_{13} & C_{23} & C_{33} & 0 & 0 & C_{36}\\ 0 & 0 & 0 & C_{44} & C_{45} & 0\\ 0 & 0 & 0 & C_{45} & C_{55} & 0\\ C_{16} & C_{26} & C_{36} & 0 & 0 & C_{66}\end{bmatrix}\begin{bmatrix}\varepsilon_{xx}\\ \varepsilon_{yy}\\ \varepsilon_{zz}\\ \varepsilon_{yz}\\ \varepsilon_{zx}\\ \varepsilon_{xy}\end{bmatrix}. \tag{6}$$

It is assumed that the external forces system applied to the composite plate changes with time in the form

$$\sigma_{ij}=\sigma_{ij}^{n}+\frac{2z}{h}\sigma_{ij}^{m}=\left(\sigma_{ij}^{S}+\sigma_{ij}^{D}\cos\varpi t\right)+2z\left(\sigma_{ij}^{Sm}+\sigma_{ij}^{Dm}\cos\varpi t\right),\left(i,j=x,y,z\right). \tag{7}$$

Here, σ_{ij}^{n} is the periodic normal or shear stress, and σ_{ij}^{S} and σ_{ij}^{D} are the corresponding static and dynamic components; σ_{ij}^{m} is the periodic pure bending or torsion stress, and σ_{ij}^{Sm} and σ_{ij}^{Dm} are the associated static and dynamic components; ϖ is the disturbing frequency of the periodic loading. Inserting Eqs. (3)-(7) into Eq. (2), performing partial integrations, removing derivatives from the variation of the displacements, and grouping terms by the displacement variations leads to the following governing equations for the composite plate:

$$Q_{1,x}+Q_{2,y}+\left(R_1+R_5+R_{17}\right)_{,x}+\left(S_1+S_6+S_{17}\right)_{,y}+f_x=I_1\ddot{u}_x+I_3\ddot{\xi}_x, \tag{8}$$

$$Q_{2,x}+Q_{3,y}+\left(R_9+R_{13}+R_{21}\right)_{,x}+\left(S_9+S_{13}+S_{21}\right)_{,y}+f_y=I_1\ddot{u}_y+I_3\ddot{\xi}_y, \tag{9}$$

$$Q_{4,x}+Q_{5,y}+(R_{30}+R_{33}+R_{25})_{,x}+(S_{30}+S_{33}+S_{25})_{,y}+f_z=I_1\ddot{w}+I_3\ddot{\xi}_z, \tag{10}$$

$$Q_{6,x}+Q_{7,y}-Q_4+(R_2+R_6+R_{18})_{,x}+(S_2+S_6+S_{18})_{,y}-(U_1+U_5+W_1)+m_x=I_3\ddot{\varphi}_x+I_5\ddot{\phi}_x, \tag{11}$$

$$Q_{7,x}+Q_{8,y}-Q_5+(R_{10}+R_{14}+R_{22})_{,x}+(S_{10}+S_{14}+S_{22})_{,y}-(U_9+U_{13}+W_5)+m_y=I_3\ddot{\varphi}_y+I_5\ddot{\phi}_y, \tag{12}$$

$$Q_{9,x}+Q_{10,y}-Q_{11}+(R_{31}+R_{34}+R_{36})_{,x}+(S_{31}+S_{34}+S_{36})_{,y}-(V_1+V_4+W_9)+m_z=I_3\ddot{\varphi}_z, \tag{13}$$

$$Q_{12,x}+Q_{13,y}-2Q_9+(R_3+R_7+R_{19})_{,x}+(S_3+S_7+S_{19})_{,y}-2(U_2+U_6+W_2)+n_x=I_3\ddot{u}_x+I_5\ddot{\xi}_x, \tag{14}$$

$$Q_{13,x}+Q_{14,y}-2Q_{10}+(R_{11}+R_{15}+R_{23})_{,x}+(S_{11}+S_{15}+S_{23})_{,y}+n_y=I_3\ddot{u}_y+I_5\ddot{\xi}_y, \tag{15}$$

$$Q_{15,x}+Q_{16,y}-2Q_{17}+(R_{32}+R_{35}+R_{27})_{,x}+(S_{32}+S_{35}+S_{27})_{,y}-2(V_2+V_5+W_{10})+n_z=I_3\ddot{w}+I_5\ddot{\xi}_z, \tag{16}$$

$$Q_{18,x}+Q_{19,y}-3Q_{15}+(R_4+R_8+R_{20})_{,x}$$
$$+(S_4+S_8+S_{20})_{,y}-3(U_3+U_7+W_3)+q_x = I_5\ddot{\varphi}_x+I_7\ddot{\phi}_x, \tag{17}$$
$$Q_{19,x}+Q_{20,y}-3Q_{16}+(R_{12}+R_{16}+R_{24})_{,x}$$
$$+(S_{12}+S_{16}+S_{24})_{,y}-3(U_{11}+U_{15}+W_7)+q_y = I_5\ddot{\varphi}_y+I_7\ddot{\phi}_y, \tag{18}$$

where Q are related to the strain–displacement of the composite plate; the terms $R,S,U,V,$ and W are arbitrary external forces associated with initial stresses; I are the inertia-related terms; f_x, f_y, f_z, m_x, m_y, m_z, n_x, n_y, n_z, q_x, and q_y are body forces and lateral loads. More detailed information about the relevant parameters in Eqs. (8)-(18) is given in the Appendix, which is recalled and rewritten from [26].

3. Solution Procedure

It is difficult to give results for all cases, because the dynamic behavior of the composite plate studied in this paper is affected by too many parameters. Therefore, the case studied is the dynamics of a simply supported cross-ply laminated plate subjected to a spatially uniform periodic in-plane stress system, which is composed of a pulsating uniaxial stress and a pure bending stress. The lateral external load and body force are set to zero. Therefore, the periodic stress system (7) becomes

$$\sigma_{xx}=\sigma_{xx}^{n}+\frac{2z\sigma_{xx}^{m}}{h}=\sigma_n+2z\sigma_m/h. \tag{19}$$

Here, $\sigma_n=\sigma^S+\sigma^D\cos\varpi t$ and $\sigma_m=\sigma^{Sm}+\sigma^{Dm}\cos\varpi t$ are the normal and bending stresses, respectively, σ^S, σ^{Sm}, and σ^D, σ^{Dm} are the corresponding static dynamic components assumed to be constants. The nonzero periodic loads are $N_{xx}=h\sigma_n$, $M_{xx}=Sh^2\sigma_m/6$, $M_{xx}^*=h^3\sigma_n/12$, $P_{xx}=Sh^4\sigma_n/40$, $P_{xx}^*=h^5\sigma_n/80$, $R_{xx}=Sh^6\sigma_n/224$, and $R_{xx}^*=h^7\sigma_n/448$. In the ratio $S=\sigma_m/\sigma_n$, σ_m and σ_n are periodic bending normal stresses.

Regarding the composite plate with simply supported edges, displacement field (20) that satisfying geometric boundary conditions can be expressed as follows.

$$\begin{aligned}
u_x&=\sum\sum hU_{mn}\cos(m\pi x/a)\sin(n\pi y/b),\\
u_y&=\sum\sum hV_{mn}\sin(m\pi x/a)\cos(n\pi y/b),\\
w&=\sum\sum hW_{mn}\sin(m\pi x/a)\sin(n\pi y/b),\\
\varphi_x&=\sum\sum \psi_{xmn}\cos(m\pi x/a)\sin(n\pi y/b),\\
\varphi_y&=\sum\sum \psi_{ymn}\sin(m\pi x/a)\cos(n\pi y/b),\\
\varphi_z&=\sum\sum \psi_{zmn}\sin(m\pi x/a)\sin(n\pi y/b),\\
\xi_x&=\sum\sum(\zeta_{xmn}/h)\cos(m\pi x/a)\sin(n\pi y/b),\\
\xi_y&=\sum\sum(\zeta_{ymn}/h)\sin(m\pi x/a)\cos(n\pi y/b),\\
\xi_z&=\sum\sum(\zeta_{zmn}/h)\sin(m\pi x/a)\sin(n\pi y/b),\\
\phi_x&=\sum\sum(\Phi_{xmn}/h^2)\cos(m\pi x/a)\sin(n\pi y/b),\\
\phi_y&=\sum\sum(\Phi_{ymn}/h^2)\sin(m\pi x/a)\cos(n\pi y/b).
\end{aligned} \tag{20}$$

Inserting the displacement field and periodic loads into governing equations (8)-(18), employing the Galerkin method, and grouping coefficients, the governing matrix equation of motion is obtained in the form

$$\begin{gathered}\left[M\right]\left[\ddot{\Delta}\right]+\left\{\left[C\right]+\left[G\right]\right\}\left[\Delta\right]=0\,,\\ \left\{\Delta\right\}=\left[U_{mn},V_{mn},W_{mn},\psi_{xmn},\psi_{ymn},\psi_{zmn},\zeta_{xmn},\zeta_{ymn},\zeta_{zmn},\Phi_{xmn},\Phi_{ymn}\right]^{T},\end{gathered}\tag{21}$$

where Δ is a time-dependent displacement vector of HSNT. The time-dependent displacement vector of FSDT is $\left[U_{mn},V_{mn},W_{mn},\psi_{xmn},\psi_{ymn}\right]^{T}$. [M], [C], and [G] are the inertia, elastic stiffness, and geometric stiffness matrices, respectively. Matrix equation (21) can be used to analyze the eigenvalue problems of free vibration, static buckling stability, and dynamic instability.

Neglecting the in-plane external loads and the [G] matrix and inserting $\Delta(t)=\Delta e^{i\omega t}$ into Eq. (21), Eq. (21) reduces to

$$\left\{\left[C\right]-\omega^{2}\left[M\right]\right\}\left[\Delta\right]=0\,,\tag{22}$$

which is the eigenvalue equation associated with free vibrations of the composite plate. The condition for the existence of a nonzero solution is that the determinant of the coefficient matrix has to be equal to zero, namely,

$$\left|\left[C\right]-\omega^{2}\left[M\right]\right|=0\tag{23}$$

from which the natural frequency ω can be found,

To analyze the static buckling, the matrix of inertia terms of Eq. (21) is asumed zero. The eigenvalue equation for the static buckling load N_{xx} is

$$\left\{\left[C\right]+N_{xx}\left[G\right]^{*}\right\}\left[\Delta\right]=0\,.\tag{24}$$

Likewise, the static buckling load can be obtained by equating the determinant of the coefficient matrix of Eq. (24) to zero. The nonzero periodic load N_{xx} is obtained by integrating Eq. (19), which gives that

$$N_{xx}=h\sigma_{n}=h\left(\sigma^{S}+\sigma^{D}\cos\varpi t\right)=\alpha_{S}P_{cr}+\alpha_{D}P_{cr}\cos\varpi t\tag{25}$$

where P_{cr}, α_{S}, and α_{D} are the buckling load and parameters of static and dynamic loads, respectively. Inserting Eq. (25) into Eq. (21) leads to the relation

$$\left[\mathrm{M}\right]\left[\ddot{\Delta}\right]+\left\{\left[C\right]+\alpha_{S}P_{cr}\left[G\right]+\alpha_{D}P_{cr}\left[G\right]\cos\varpi t\right\}\left[\Delta\right]=0\,,\tag{26}$$

which is a second-order ordinary differential equation of Mathieu–Hill type. Then, Bolotin's method is used to find the boundaries between the stable and the unstable regions of the parametrically excited structure through the periodic solutions of period T and $2T$ in Fourier series, where $T=2\pi/w$. The periodic solutions Δ of Eq. (26) with periods T and $2T$ can be found by Fourier series as

$$\Delta=\sum_{k=1,3,5\ldots}^{\infty}\left(a_{k}\sin\frac{k\varpi t}{2}+b_{k}\cos\frac{k\varpi t}{2}\right),\tag{27}$$

$$\Delta=\sum_{k=0,2,4\ldots}^{\infty}\left(a_{k}\sin\frac{k\varpi t}{2}+b_{k}\cos\frac{k\varpi t}{2}\right),\tag{28}$$

where a_{k} and b_{k} are arbitrary time-invariant constants. Inserting expansions (27) and (28) into Eq. (26) and grouping the sin and cosine parts, respectively, two sets of linear algebraic equations in a_{k} and b_{k} are obtained. Generally, the primary unstable region defined by the solution with a period $2T$ is much larger than the secondary unstable region defined by the solution with a period T. Therefore, the primary instability region with the period $2T$ has the greatest practical significance and

TABLE 1. Natural Frequencies of Antisymmetric Cross-Ply Square Laminated Plates with Various Numbers of Layers and Modulus Ratios. (a/b = 1, a/h = 5)

Composite	Theory	E_x/E_y			
		10	20	30	40
(0°/90°)	FSDT	6.9301	7.6934	8.3052	8.8142
	[27]	6.9156	7.6922	8.3112	8.8255
	HSNT	6.9802	7.7188	8.2815	8.7305
	[28]	6.9741	7.7140	8.2775	8.7272
$(0°/90°)_2$	FSDT	8.1590	9.6627	10.5857	11.2298
	[27]	8.1363	9.6729	10.6095	11.2635
	HSNT	8.1563	9.4760	10.2819	10.8306
	[28]	8.1482	9.4675	10.2733	10.8221
$(0°/90°)_3$	FSDT	8.4015	9.9148	10.8460	11.4825
	[27]	8.3883	9.9266	10.8723	11.5189
	HSNT	8.3939	9.8430	10.7196	11.3131
	[28]	8.3852	9.8346	10.7113	11.3051

gives a sufficiently accurate solution. Since the first-order approximation to a_1 and b_1 of the primary instability region can be solved with a sufficient accuracy, the first-order solution of the primary instability region can be obtained as

$$[C]+\alpha_S P_{cr}[G]\pm\frac{1}{2}\alpha_D P_{cr}[G]-\frac{1}{4}\varpi^2[M]=0\,. \tag{29}$$

4. Analyses and Discussion

Let us investigate the dynamic instability of composite plates based on a high-order plate theory. The material properties of laminates are E_x/E_y = open, $E_y=E_z$, $G_{xy}=G_{xz}=0.6E_y$, $G_{yz}=0.5E_y$, and $\upsilon_{xy}=\upsilon_{xz}=\upsilon_{yz}=0.25$. The current HSNT can be simplified to FSDT by neglecting the higher-order terms and introducing a shear correction factor into the resultants of shear stresses. In the following, the results obtained based on the HSNT and FSDT are presented to show the difference between the two theories. The nondimensional parameter $\Omega=\varpi b^2/h\sqrt{\rho/E_y}$ of excitation frequency and the dynamic instability index $\Omega_{DI}=100\Delta\Omega/\left(\omega_{nf}/P_{cr}\right)$ are utilized in the following study. Among them, $\omega_{nf}=\omega b^2/h\sqrt{\rho/E_y}$ and $P_{cr}=10\sigma_n b^2/E_y h^4$ are the fundamental natural frequency and critical buckling load, respectively; $\Delta\Omega=\Omega^U-\Omega^L$ is the width of the instability region bounded by the upper Ω^U and lower Ω^L excitation frequency. The dynamic instability index Ω_{DI} quantifies the instability measure through the instability area, natural frequency, and buckling load.

To verify the accuracy of the present model, some representative examples were investigated. First, the free vibration of antisymmetric cross-ply laminated plates according to FSDT and HSNT is considered. Table 1 present the natural frequencies of laminated plates with various layer numbers and modulus ratios. The frequencies calculated by the present model agree well with those by Whitney [27] and Kant [28]. It can be seen in Table 1 that the frequency increases with E_x/E_y and layer number. Second, the dynamic stability of a symmetrically four-layer cross-ply laminate plate under various static and dynamic loads was studied. Table 2 show the upper and lower excitation frequencies of the laminate plate by using the HSNT along with the results obtained by Wang [29] and Chen [30] based on the FSDT. The numerical values of HSNT were in a good agreement with those of FSDT. As seen in Table 2, with increasing dynamic load (α_S = 0), the upper excitation frequency increases but the lower one reduces. Additionally, the upper and lower excitation frequencies

TABLE 2. Excitation Frequencies for a Symmetrical Four-Layer Cross-Ply Laminated Plates with Various Static and Dynamic Load Parameters

α_S	α_D	[29]		FSDT [30]		HSNT	
		Ω^U	Ω^L	Ω^U	Ω^L	Ω^U	Ω^L
0	0	144.57	144.57	144.36	144.36	144.97	144.97
0	0.3	155.03	133.29	155.64	133.79	155.45	133.67
0	0.6	164.83	120.95	165.12	121.45	165.27	121.32
0	0.9	174.08	107.21	174.43	107.63	174.53	107.56
0	1.2	182.87	91.43	183.21	91.86	183.33	91.76
0	1.5	191.25	72.28	191.75	72.62	191.73	72.60
0.2	0.06	131.71	126.86	132.12	127.26	132.09	127.23
0.4	0.12	117.45	106.24	117.96	106.82	117.80	106.58
0.6	0.18	101.20	80.49	101.84	81.10	101.53	80.81
0.8	0.24	81.78	40.89	82.31	41.32	82.10	41.27

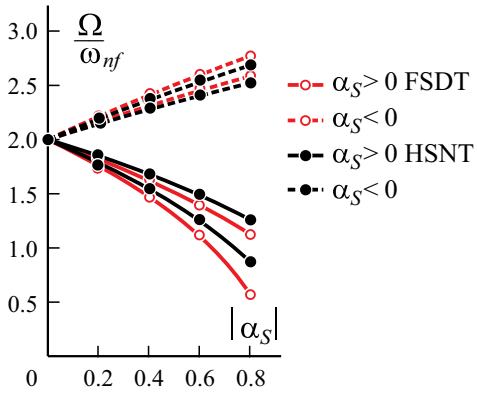

Fig. 1. Effect of static loads on Ω / ω_{nf} ($a/b = 1$, $a/h = 10$, $n = 1$, $\alpha_D / |\alpha_S| = 0.3$, S =0, $\alpha_S < 0$ tensile load, and $\alpha_S > 0$ compressive load).

decrease as both the static and dynamic loads increase. The results obtained by the present method match well with other research results. It verifies the reliability and accuracy of the present computer program.

Figure 1 presents the effect of static loading on the ratio Ω / ω_{nf} excitation frequencies. The plot shows that excitation frequency first appears near 2 at $\alpha_S = \alpha_D = 0$. It can be observed that, as the compressive static ($\alpha_S < 0$) load increases, the upper and lower excitation frequency ratios decrease. However, an increasing tensile static load leads to an opposite effect. The width between boundaries of both excitation frequency ratios increases with growing static load parameter. Meanwhile, the static compression load reduces the stiffness of the plate, so it has a more significant influence on the boundary width than the static tension load. The effect of dynamic loads on the excitation frequency ratio of the instability region is shown in Fig. 2. Under a compressive static load, the initial excitation frequency ratio is smaller than 2 ($\alpha_D = 0$), while under a tensile static load, the initial excitation frequency ratio is greater than 2. An increase in the dynamic load parameter increases the upper excitation frequency ratio, reduces the lower one, and enlarges the width of the unstable region. The dynamic load parameter has a greater influence on the excitation frequency ratio than the static load parameter. As shown in Figs. 1 and 2, the width of the unstable region obtained by FSDT is larger than that given by HSNT, especially under a compressive static load.

The effects of layer number and modulus ratio on the excitation frequency, instability region, and dynamic instability index of antisymmetric cross-ply laminated plates under the static load parameter $\alpha_S = 0.5$ and load parameter ratio

TABLE 3. Excitation Frequencies, Instability Regions, and Dynamic Instability Index of Antisymmetric Cross-Ply Laminated Plates with Various Numbers of Layer and Modulus Ratios ($a/b = 1$, $a/h = 5$, $\alpha_S = 0.5$, $\alpha_D / \alpha_S = 0.3$)

Composite	A	Theory	E_x/E_y			
			10	20	30	40
(0°/90°)	Ω^U	FSDT	10.5100	11.6677	12.5955	13.3674
		HSNT	10.8081	12.0573	13.0216	13.7978
	Ω^L	FSDT	9.0358	10.0310	10.8287	11.4924
		HSNT	9.4476	10.6102	11.5145	12.2460
	$\Delta\Omega^U$	FSDT	1.4743	1.6367	1.7668	1.8751
		HSNT	1.3605	1.4471	1.5071	1.5518
	Ω_{DI}	FSDT	1.0929	0.8868	0.7610	0.6756
		HSNT	1.0471	0.8462	0.7286	0.6512
$(0°/90°)_2$	Ω^U	FSDT	12.4496	14.6543	16.0539	17.0309
		HSNT	12.3692	14.3698	15.5911	16.4225
	Ω^L	FSDT	10.7032	12.5987	13.8020	14.6419
		HSNT	10.6338	12.3532	13.4026	14.1169
	$\Delta\Omega^U$	FSDT	1.7464	2.0556	2.2520	2.3890
		HSNT	1.7354	2.0166	2.1885	2.3057
	Ω_{DI}	FSDT	3.1158	2.2488	1.8737	1.6650
		HSNT	3.1566	2.3391	1.9872	1.7912
$(0°/90°)_3$	Ω^U	FSDT	12.7415	15.0365	16.4488	17.4141
		HSNT	12.7296	14.9267	16.2554	17.1548
	Ω^L	FSDT	10.9542	12.9273	14.1415	14.9714
		HSNT	10.9437	12.8321	13.9740	14.7468
	$\Delta\Omega^U$	FSDT	1.7873	2.1092	2.3073	2.4427
		HSNT	1.7859	2.0945	2.2814	2.4080
	Ω_{DI}	FSDT	2.9746	2.1359	1.7848	1.5925
		HSNT	2.9803	2.1677	1.8280	1.6414

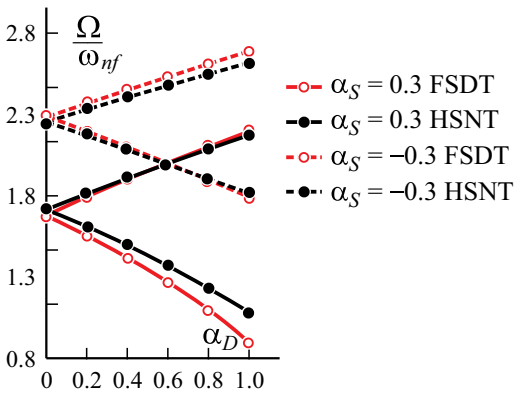

Fig. 2. Effect of dynamic loads on Ω / ω_{nf} ($a/b = 1$, $a/h = 10$, $n = 1$, $S = 0$, $\alpha_D / |\alpha_S| = 0.3$.

$\alpha_D / \alpha_S = 0.3$ are presented in Table 3. As the modulus ratio increases, the excitation frequencies and instability region grow, but the dynamic instability index diminishes. With increasing number of layers, the excitation frequencies and un-

TABLE 4. Effect of the Modulus Ratio E_x / E_y on the Excitation Frequencies, Instability Regions, and Dynamic Instability Index of Laminated Plates under Various Static Loads (a/b = 1, a/h = 5, n =1, S =0, α_D / α_S = 0.3)

E_x/E_y	A	Theory	α_S					
			0	0.2	0.4	0.6	0.8	Diff.*, %
10	Ω^U	FSDT	13.8602	12.6273	11.2601	9.7022	7.8405	6.27
		HSNT	13.9604	12.7930	11.5078	10.0597	8.3646	
	Ω^L	FSDT	13.8602	12.1623	10.1852	7.7170	3.9202	22.93
		HSNT	13.9604	12.3547	10.5064	8.2541	5.0868	
	$\Delta\Omega^U$	FSDT	0	0.4650	1.0750	1.9851	3.9203	19.60
		HSNT	0	0.4383	1.0014	1.8057	3.2778	
	Ω_{DI}	FSDT	0	0.3447	0.7969	1.4717	2.9063	15.20
		HSNT	0	0.3374	0.7708	1.3898	2.5228	
20	Ω^U	FSDT	15.3869	14.0181	12.5003	10.7708	8.7041	8.05
		HSNT	15.4376	14.1825	12.8050	11.2601	9.4665	
	Ω^L	FSDT	15.3869	13.5019	11.3070	8.5670	4.3520	28.58
		HSNT	15.4376	13.7121	11.7356	9.3503	6.0935	
	$\Delta\Omega^U$	FSDT	0	0.5162	1.1934	2.2038	4.3521	29.03
		HSNT	0	0.4704	1.0693	1.9099	3.3730	
	Ω_{DI}	FSDT	0	0.2797	0.6466	1.1941	2.3582	19.57
		HSNT	0	0.2750	0.6253	1.1168	1.9723	
40	Ω^U	FSDT	17.6284	16.0603	14.3214	12.3399	9.9722	9.60
		HSNT	17.4611	16.0961	14.6042	12.9414	11.0306	
	Ω^L	FSDT	17.6284	15.4689	12.9542	9.8151	4.9862	33.96
		HSNT	17.4611	15.5859	13.4518	10.9078	7.5506	
	$\Delta\Omega^U$	FSDT	0	0.5914	1.3672	2.5248	4.9860	43.27
		HSNT	0	0.5103	1.1524	2.0335	3.4801	
	Ω_{DI}	FSDT	0	0.2131	0.4926	0.9097	1.7966	23.03
		HSNT	0	0.2141	0.4836	0.8533	1.4603	

*Percentage difference of the absolute value of (FSDT-HSNT)/HSNT at α_S = 0.8

stable region grow, but the dynamic instability index first increases and then decreases. For plates with different numbers of layers and modulus ratios, there is no obvious difference between the values obtained based on the HSNT and FSDT for the respective excitation frequency, instability area, and dynamic instability index, except for the instability area of the plate with two layer laminates and higher modulus ratio. The size of the instability region evaluated by FSDT is greater than that of HSNT, and the difference increases with increasing modulus ratio and decreasing layer number.

Tables 4 and 5 show the effects of static and dynamic loads on the dynamic instability characteristics of laminated plates with various modulus ratio. As can be seen, when the static or dynamic load increases, both the instability region and dynamic instability index increase. Thus, the composite plate is more dynamically unstable when it is subjected to a high static or dynamic load. An increase in the modulus ratio enhances the rigidity of the laminated plate, decreases the dynamic instability index and make the laminated plate dynamically more stable. An increase in the static or dynamic load enhances the difference between calculation results of FSDT and HSNT, which is most obvious at low excitation frequencies and an unstable region. It can be seen in Tables 4 and 5 that the difference between FSDT and HSNT results caused by the compressive static load is significantly greater than by a dynamic load. This is because, when studying the influence of a dynamic load in Table 5, the static load applied was relatively small. In the case of a large static load, an increasing

TABLE 5. Effect of the Modulus Ratio E_x / E_y on the Excitation Frequencies. Instability Regions. and Dynamic Instability Index of Laminated Plates under Various Dynamic Loads ($a/b = 1$. $a/h = 5$. $n = 1$. $S = 0$. $\alpha_S = 0.1$)

E_x/E_y	A	Theory	α_D					
			0	0.4	0.8	1.2	1.6	Diff.*, %
10	Ω^U	FSDT	13.1490	14.5368	15.8031	16.9753	18.0716	0.48
		HSNT	13.2861	14.6036	15.8116	16.9337	17.9859	
	Ω^L	FSDT	13.1490	11.5963	9.8007	7.5916	4.3830	19.37
		HSNT	13.2861	11.8228	10.1506	8.1420	5.4360	
	$\Delta\Omega^U$	FSDT	0	2.9404	6.0025	9.3837	13.6886	9.07
		HSNT	0	2.7808	5.6610	8.7917	12.5499	
	Ω_{DI}	FSDT	0	2.1799	4.4499	6.9566	10.1480	5.06
		HSNT	0	2.1403	4.3570	6.7666	9.6592	
20	Ω^U	FSDT	14.5973	16.1379	17.5438	18.8450	20.0621	1.41
		HSNT	14.7123	16.1304	17.4335	18.6457	19.7838	
	Ω^L	FSDT	14.5973	12.8736	10.8801	8.4277	4.8657	24.47
		HSNT	14.7123	13.1421	11.3568	9.2326	6.4424	
	$\Delta\Omega^U$	FSDT	0	3.2643	6.6636	10.4173	15.1964	13.90
		HSNT	0	2.9883	6.0766	9.4131	13.3414	
	Ω_{DI}	FSDT	0	1.7688	3.6107	5.6446	8.2342	5.55
		HSNT	0	1.7473	3.5532	5.5042	7.8012	
40	Ω^U	FSDT	16.7238	18.4888	20.0995	21.5903	22.9846	3.47
		HSNT	16.6717	18.2163	19.6397	20.9668	22.2147	
	Ω^L	FSDT	16.7238	14.7490	12.4652	9.6555	5.5747	29.43
		HSNT	16.6717	14.9686	13.0450	10.7836	7.8994	
	$\Delta\Omega^U$	FSDT	0	3.7398	7.6343	11.9348	17.4099	21.62
		HSNT	0	3.2477	6.5947	10.1832	14.3153	
	Ω_{DI}	FSDT	0	1.3628	2.7508	4.5004	6.4732	6.11
		HSNT	0	1.3458	2.7051	4.3868	6.1005	

*Percentage difference of the absolute value of (FSDT-HSNT)/HSNT at $\alpha_D = 1.6$

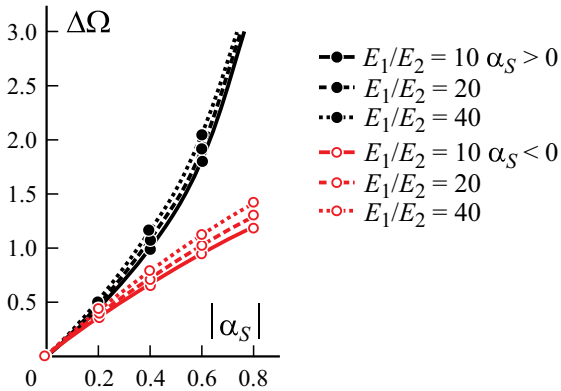

Fig. 3. Effect of modulus ratios on the instability regions at various static load types. ($a/b = 1$, $a/h = 5$, $n = 1$, $S = 0$, $\alpha_D / |\alpha_S| = 0.3$).

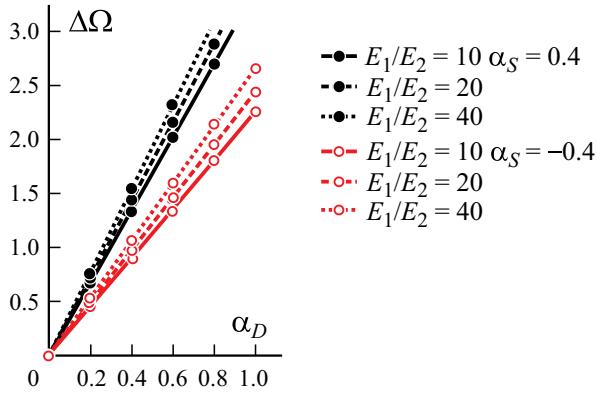

Fig. 4. Effect of modulus ratios on the instability region at various dynamic loads. ($a/b = 1$, $a/h = 5$, $n = 1$, $S = 0$).

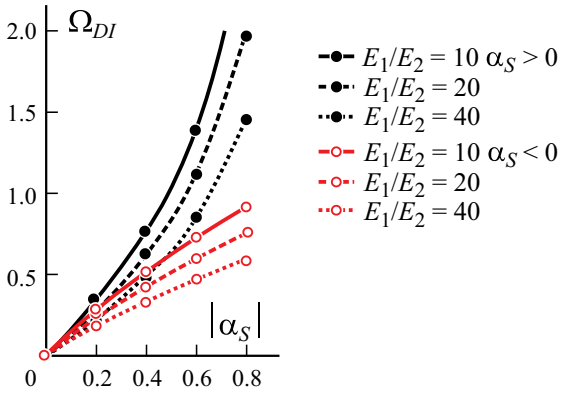

Fig. 5. Effect of modulus ratios on the dynamic instability index at various static load types. ($a/b = 1$, $a/h = 5$, $n = 1$, $S = 0$, $\alpha_D / |\alpha_S| = 0.3$).

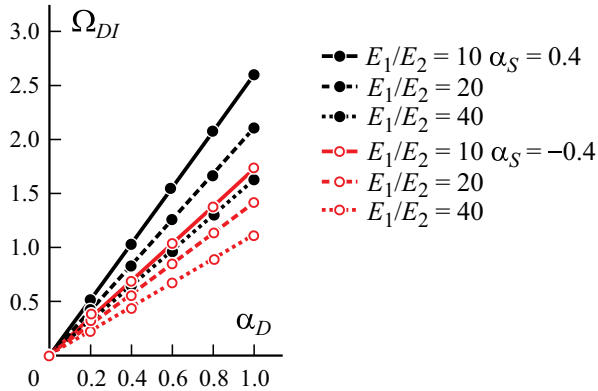

Fig. 6. Effect of modulus ratios on the dynamic instability index at various dynamic loads ($a/b = 1$, $a/h = 5$, $n = 1$, $S = 0$).

dynamic load also increases the difference between FSDT and HSNT results. Figures 3 and 4 present the effects of modulus ratios on the instability regions of laminated plates under various static and dynamic loads, based on the HSNT. Whether a laminated plate is under a tensile or compressive static load, increasing the modulus ratio always enhances the instability region. The unstable region of a laminated plate under a compressive load is larger than that under a tensile load, and as

TABLE 6. Effect of the Load Parameter Ratio on the Excitation Frequencies. Instability Regions. and Dynamic Instability Index of Laminated Plates under Various Dynamic Loads ($a/b = 1$. $a/h = 5$. $n = 1$. $S = 0$. $E_x / E_y = 40$)

α_D/α_S	A	Theory	α_S			
			–0.6	–0.3	0.3	0.6
0.2	Ω^U	FSDT	22.7126	20.3301	15.0617	11.9562
		HSNT	21.9708	19.8444	15.2362	12.6252
	Ω^L	FSDT	21.8763	19.8662	14.4295	10.2791
		HSNT	21.2222	19.4329	14.6961	11.2723
	$\Delta\Omega^U$	FSDT	0.8363	0.4639	0.6322	1.6771
		HSNT	0.7485	0.4116	0.5401	1.3529
	Ω_{DI}	FSDT	0.3014	0.1671	0.2278	0.6043
		HSNT	0.3141	0.1727	0.2266	0.5677
0.5	Ω^U	FSDT	23.3202	20.6711	15.5190	13.0736
		HSNT	22.5159	20.1476	15.6290	13.5516
	Ω^L	FSDT	21.2274	19.5111	13.9365	8.8143
		HSNT	20.6430	19.1184	14.2777	10.1398
	$\Delta\Omega^U$	FSDT	2.0928	1.1601	1.5825	4.2593
		HSNT	1.8728	1.0293	1.3514	3.4118
	Ω_{DI}	FSDT	0.7541	0.4180	0.5702	1.5347
		HSNT	0.7859	0.4319	0.5671	1.4317
1	Ω^U	FSDT	24.2991	21.2274	16.2526	14.7490
		HSNT	23.3961	20.6430	16.2627	14.9686
	Ω^L	FSDT	20.0995	18.9044	13.0736	5.5747
		HSNT	19.6397	18.5824	13.5516	7.8994
	$\Delta\Omega^U$	FSDT	4.1996	2.3230	3.1790	9.1743
		HSNT	3.7564	2.0606	2.7111	7.0693
	Ω_{DI}	FSDT	1.5132	0.8371	1.1455	3.3057
		HSNT	1.5763	0.8647	1.1377	2.9664

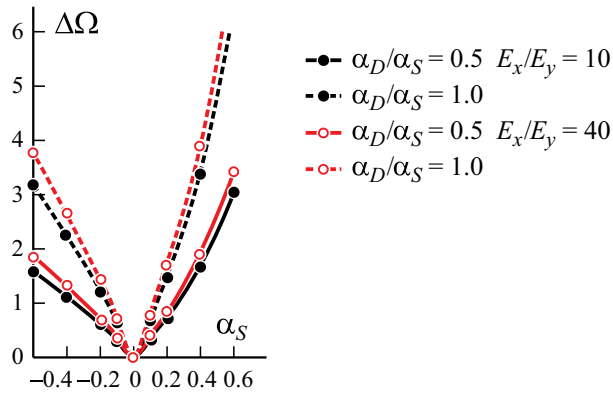

Fig. 7. Effect of the load parameter ratio on the instability region at various static loads ($a/b = 1$, $a/h = 5$, $n = 1$, $S = 0$).

the magnitude of the applied load increases, the difference between them becomes greater. The effects of modulus ratios on the dynamic instability index are presented in Figs. 5 and 6. As is seen, increasing the modulus ratio decreases the dynamic

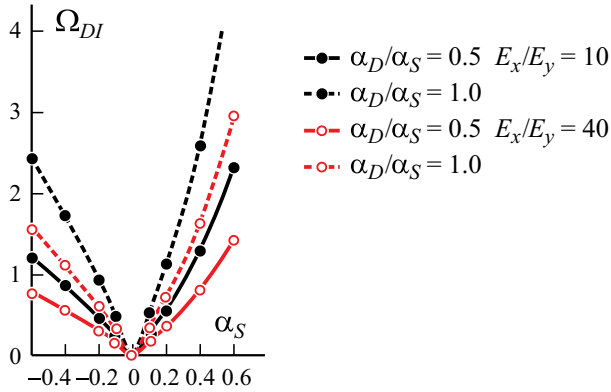

Fig. 8. Effect of the load parameter ratio on the dynamic instability index at various static loads ($a/b = 1$, $a/h = 5$, $n = 1$, $S = 0$).

TABLE 7. Effect of the Bending Stress Parameter on the Excitation Frequencies, Instability Regions and Dynamic Instability Index of Laminated Plates under Various Compressive Loads ($a/b = 1$, $a/h = 5$, $n = 1$, $E_x / E_y = 40$, $\alpha_D / \alpha_S = 0.3$)

S	A	Theory	α_S				
			0	0.15	0.3	0.45	0.6
0	Ω^U	FSDT	17.6284	16.4663	15.2157	13.8526	12.3399
		HSNT	17.4611	16.4480	15.3683	14.2067	12.9414
	Ω^L	FSDT	17.6284	16.0361	14.2671	12.2451	9.8151
		HSNT	17.4611	16.0752	14.5580	12.8630	10.9078
	$\Delta\Omega^U$	FSDT	0	0.4303	0.9486	1.6075	2.5248
		HSNT	0	0.3728	0.8103	1.3437	2.0335
	Ω_{DI}	FSDT	0	0.1550	0.3418	0.5792	0.9097
		HSNT	0	0.1564	0.3400	0.5638	0.8533
5	Ω^U	FSDT	17.6284	16.4644	15.2075	13.8325	12.2996
		HSNT	17.4611	16.4401	15.3317	14.1153	12.7599
	Ω^L	FSDT	17.6284	16.0325	14.2511	12.2033	9.7219
		HSNT	17.4611	16.0598	14.4858	12.6749	10.5051
	$\Delta\Omega^U$	FSDT	0	0.4319	0.9564	1.6292	2.5777
		HSNT	0	0.3803	0.8459	1.4404	2.2548
	Ω_{DI}	FSDT	0	0.1556	0.3446	0.5870	0.9288
		HSNT	0	0.1596	0.3550	0.6044	0.9462
10	Ω^U	FSDT	17.6284	16.4588	15.1830	13.7715	12.1768
		HSNT	17.4611	16.4138	15.2157	13.8275	12.1843
	Ω^L	FSDT	17.6284	16.0219	14.2031	12.0758	9.4325
		HSNT	17.4611	16.0099	14.2587	12.0776	9.1641
	$\Delta\Omega^U$	FSDT	0	0.4369	0.9799	1.6957	2.7444
		HSNT	0	0.4040	0.9570	1.7500	3.0202
	Ω_{DI}	FSDT	0	0.1574	0.3531	0.6110	0.9889
		HSNT	0	0.1695	0.4016	0.7343	1.1674

instability index, which is the opposite of the influence of the modulus ratio on the instability region. The influence of a static load on the dynamic instability index is similar to that on the instability region, as is seen in Figs. 3 and 4.

TABLE 8 Effect of the Bending Stress Parameter on the Excitation Frequencies, Instability Regions and Dynamic Instability Index of Laminated Plates under Various Dynamic Loads ($a/b = 1$, $a/h = 5$, $n = 1$, $E_x / E_y = 40$, $\alpha_S = 0.3$)

S	A	Theory	α_D				
			0	0.2	0.4	0.6	0.8
0	Ω^U	FSDT	14.7490	15.0617	15.3681	15.6685	15.9632
		HSNT	14.9686	15.2362	15.4992	15.7578	16.0122
	Ω^L	FSDT	14.7490	14.4295	14.1028	13.7683	13.4254
		HSNT	14.9686	14.6961	14.4185	14.1354	13.8466
	$\Delta\Omega^U$	FSDT	0	0.6322	1.2654	1.9002	2.5378
		HSNT	0	0.5401	1.0807	1.6224	2.1657
	Ω_{DI}	FSDT	0	0.2278	0.4559	0.6847	0.9144
		HSNT	0	0.2266	0.4535	0.6812	0.9088
5	Ω^U	FSDT	14.7374	15.0525	15.3610	15.6631	15.9593
		HSNT	14.9160	15.1947	15.4673	15.7340	15.9953
	Ω^L	FSDT	14.7374	14.4151	14.0852	13.7471	13.4003
		HSNT	14.9160	14.6309	14.3390	14.0397	13.7328
	$\Delta\Omega^U$	FSDT	0	0.6374	1.2758	1.9160	2.5590
		HSNT	0	0.5638	1.1283	1.6943	2.2625
	Ω_{DI}	FSDT	0	0.2297	0.4597	0.6904	0.9221
		HSNT	0	0.2366	0.4735	0.7110	0.9494
10	Ω^U	FSDT	14.7023	15.0247	15.3394	15.6470	15.9477
		HSNT	14.7501	15.0632	15.3656	15.6579	15.9406
	Ω^L	FSDT	14.7023	14.3716	14.0322	13.6833	13.3243
		HSNT	14.7501	14.4255	14.0887	13.7388	13.3746
	$\Delta\Omega^U$	FSDT	0	0.6531	1.3072	1.9636	2.6234
		HSNT	0	0.6377	1.2769	1.9191	2.5660
	Ω_{DI}	FSDT	0	0.2353	0.4710	0.7075	0.9453
		HSNT	0	0.2676	0.5358	0.8053	1.0768

In addition, a compressive static load increases the dynamic instability index more than a tensile static load, which means that a compressive load increases the instability of the laminated plate more than a tensile one.

The effect of the load parameter ratio α_D / α_S on the excitation frequency, instability region, and dynamic instability index of the laminated plates under different static loads is illustrated in Table 6. As the load parameter ratio increases, the upper excitation frequency, instability region and dynamic instability index increase, but the lower excitation frequency shows a reverse trend. When the magnitude of the static load in compression or tension increases, the instability region and the dynamic instability index increase. As can be seen in Table 6, the difference between results of FSDT and HSNT increases with the increasing magnitude of the static load. When a laminated plate with a high load parameter ratio is subjected to a high compressive static load, the discrepancy between the two theories becomes more pronounced. Variation trends of the instability region and dynamic instability index against the static loads for the laminated plates with different load parameter ratios and modulus ratios based on HSNT are presented in Figs. 7 and 8, respectively. At various load parameter ratios, the influence of the compressive load on the instability area and dynamic instability index is greater than that of the tensile load. Regardless the value of the load parameter ratio, an increase in the modulus ratio increases the instability region, but decreases the dynamic instability index.

Tables 7 and 8 show the effect of bending stress on the dynamic instability of laminated plates subjected to various static and dynamic loads. With increasing bending stress ratio, the excitation frequency decreases, but the instability region

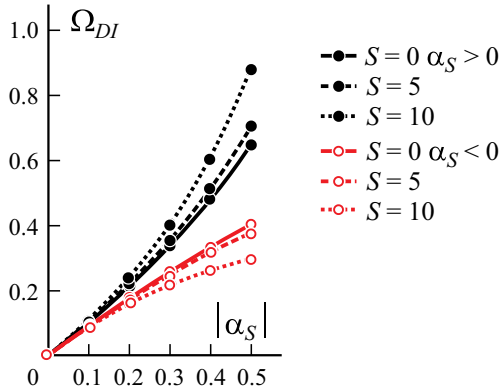

Fig. 9. Effect of the bending stress parameter on the dynamic instability index at various static loads ($a/b = 1$, $a/h = 5$, $E_x / E_y = 40$, $n = 1$, $\alpha_D / |\alpha_S| = 0.3$).

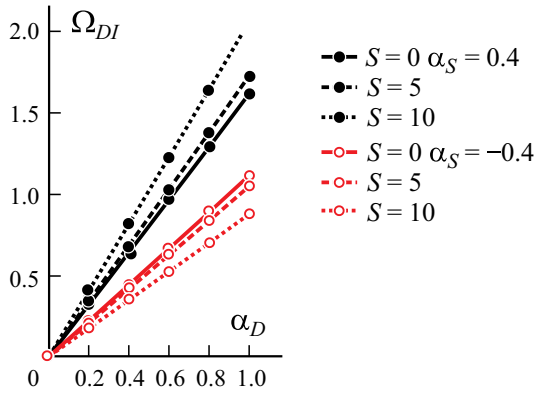

Fig. 10. Effect of the bending stress parameter on the dynamic instability index at various dynamic loads ($a/b = 1$, a/$h = 5$, $E_x / E_y = 40$, $n = 1$, $\alpha_S = 0.1$).

and dynamic instability index increase. However, the effect of the bending stress ratio is small. As the bending stress ratio increases, the difference between the calculates results based on FSDT and HSNT decreases for the excitation frequency and the unstable region and increases for the dynamic instability index. Meanwhile, the greater the bending stress ratio, the more obvious the difference between the results of FSDT and HSNT for the dynamic instability index. For example, for laminated plates with a bending stress $S = 10$ and load parameters $\alpha_D / \alpha_S = 0.3$ and $\alpha_S \geq 0.3$, or $\alpha_S = 0.3$ and $\alpha_D \geq 0.2$, the difference between the dynamic instability indices obtained by FSDT and HSNT exceeds 10%. The plots of the bending stress ratio versus the dynamic instability index for the laminated plates under different static and dynamic loads based on the HSNT are shown in Figs. 9 and 10. The results reveal that, when a laminated plate is under a higher bending stress ratio, the compressive static load has a greater hardening effect on the dynamic instability index , but the tensile static load has a reverse effect. In addition, it can be found that the difference between the calculated results under the respective tensile and compressive static load with the same magnitude becomes greater when the bending stress increases. Hence, the laminated plate is more dynamically stable, because it is under a tensile load and a higher bending stress.

5. Conclusions

The dynamic behavior of laminate plates under a periodic load based on the higher order plate theory has been described and examined. From the results obtained, the following conclusions can be drawn.

1. The static and, dynamic loads and the modulus ratio have a significant effect on the excitation frequency, instability region, and dynamic instability index. The bending stress has only a slight influence.

2. As the modulus ratio decreases under a static load in tension or compression, the instability region increases and the dynamic instability index decreases. Under a static compressive load, the bending stress enhances the instability region and the dynamic instability index. However, under a static tensile load, the bending stress has an opposite effect.

3. As the static load, dynamic load or the modulus ratio increases, the difference between the results by FSDT and HSNT becomes more pronounced. This is especially significant for laminated plates under a compressing static load. The HSNT theory has an important influence on the instability region and dynamic instability, especially for laminated plates with a high modulus ratio, bending stress, and static and dynamic loads.

Appendix

Expressions of Q.

$$\begin{bmatrix} [X_1] \\ [X_2] \\ Q_{11} \\ [X_3] \\ Q_{17} \\ [X_4] \end{bmatrix} = \begin{bmatrix} [A_1] & [B_1] & [A_2] & [D_1] & 2[B_2] & [E_1] \\ [B_1] & [D_1] & [B_2] & [E_1] & 2[D_2] & [F_1] \\ [A_3] & [B_3] & A_{33} & [D_3] & 2B_{33} & [E_3] \\ [D_1] & [E_1] & [D_2] & [F_1] & 2[E_2] & [G_1] \\ [B_3] & [D_3] & B_{33} & [E_3] & 2D_{33} & [F_3] \\ [E_1] & [F_1] & [E_2] & [G_1] & 2[F_2] & [H_1] \end{bmatrix} \begin{bmatrix} [T_1] \\ [T_2] \\ [\varphi_z] \\ [T_3] \\ [\xi_z] \\ [T_4] \end{bmatrix},$$

$$\begin{bmatrix} [[X_5]] \\ [[X_6]] \\ [[X_7]] \end{bmatrix} = \begin{bmatrix} [A_4] & [A_4] & [B_4] & 2[B_4] & [D_4] & 3[D_4] \\ [B_4] & [B_4] & [D_4] & 2[D_4] & [E_4] & 3[E_4] \\ [D_4] & [D_4] & [E_4] & 2[E_4] & [F_4] & 3[F_4] \end{bmatrix} \begin{bmatrix} [[X_8]] \end{bmatrix},$$

where

$$[X_1]=[Q_1Q_2Q_3]^T,\ [X_2]=[Q_6Q_7Q_8]^T,\ [X_3]=[Q_{12}Q_{13}Q_{14}]^T,$$

$$[X_4]=[Q_{18}Q_{19}Q_{20}]^T,\ [X_5]=[Q_4Q_5]^T,\ [X_6]=[Q_9Q_{10}]^T,\ [X_7]=[Q_{15}Q_{16}]^T,$$

$$[[X_8]] = [[T_5][T_6][T_7][T_8][T_9][T_{10}]]^T,$$

$$[T_1]=\left[u_{x,x}u_{x,y}u_{y,x}u_{y,y}\right]^T,\ [T_2]=\left[\varphi_{x,x}\varphi_{x,y}\varphi_{y,x}\varphi_{y,y}\right]^T,\ [T_3]=\left[\xi_{x,x}\xi_{x,y}\xi_{y,x}\xi_{y,y}\right]^T,$$

$$[T_4]=\left[\phi_{x,x}\phi_{x,y}\phi_{y,x}\phi_{y,y}\right]^T,\ [T_5]=\left[w_{,x}w_{,y}\right]^T,\ [T_6]=\left[\varphi_x\varphi_y\right]^T,\ [T_7]=\left[\varphi_{z,x}\varphi_{z,y}\right]^T,$$

$$[T_8]=\left[\xi_x\xi_y\right]^T,\ [T_9]=\left[\xi_{z,x}\xi_{z,y}\right]^T,\ [T_{10}]=\left[\phi_x\phi_y\right]^T,$$

Matrices [A_i], [B_i], [D_i], [E_i], [F_i], [G_i], and [H_i] can be obtained by the following expressions.

$$\left[\Gamma_1\right]=\begin{bmatrix}\Gamma_{11} & \Gamma_{16} & \Gamma_{16} & \Gamma_{12}\\ \Gamma_{16} & \Gamma_{66} & \Gamma_{66} & \Gamma_{26}\\ \Gamma_{12} & \Gamma_{26} & \Gamma_{26} & \Gamma_{22}\end{bmatrix},\ \Gamma = A,B,D,E,F,G^{*},H\ ,$$

$$\left[\Gamma_2\right]=\left[\Gamma_{13}\ \Gamma_{36}\ \Gamma_{23}\right]^{T},\ \Gamma = A,B,D,E,F\ ,$$

$$\left[\Gamma_3\right]=\left[\Gamma_{13}\ \Gamma_{36}\ \Gamma_{36}\ \Gamma_{23}\right],\ \Gamma = A,B,D,E,F\ ,$$

$$\left[\Gamma_4\right]=\begin{bmatrix}\Gamma_{55} & \Gamma_{45}\\ \Gamma_{45} & \Gamma_{55}\end{bmatrix},\ \Gamma = A,B,D,E,F\ ,$$

where

$$(\ A_{ij},B_{ij},D_{ij},E_{ij},F_{ij},G_{ij},H_{ij}\ )=\int C_{ij}\left(1,\ z,\ z^2,\ z^3,\ z^4,\ z^5,\ z^6\right)dz\ \ (i,j=1,\ 2,\ 3,\ 4,\ 5,\ 6\ ).$$

Here, C_{ij} is the stiffness matrix of elastic constants. $A_{ij},B_{ij},D_{ij},E_{ij},F_{ij},G_{ij},$ and H_{ij} are the matrices of laminate stiffness coefficients. The expressions of terms $R,S,U,V,$ and W are

$$\left\{O_1\right\}=\left[\Sigma_{xx}\right]\left\{\Delta_{xx}\right\},\left\{O_2\right\}=\left[\Sigma_{xy}\right]\left\{\Delta_{xy}\right\}\ ,\left\{O_3\right\}=\left[\Sigma_{xx}\right]\left\{\Delta_{yx}\right\},$$

$$\left\{O_4\right\}=\left[\Sigma_{xy}\right]\left\{\Delta_{yy}\right\},\left\{O_5\right\}=\left[\Sigma_{yy}\right]\left\{\Delta_{xy}\right\}\ ,\left\{O_6\right\}=\left[\Sigma_{xy}\right]\left\{\Delta_{xx}\right\},$$

$$\left\{O_7\right\}=\left[\Sigma_{yy}\right]\left\{\Delta_{yy}\right\},\left\{O_8\right\}=\left[\Sigma_{xy}\right]\left\{\Delta_{yx}\right\}\ ,\left\{O_9\right\}=\left[\Sigma_{xz}\right]\left\{\Delta_{zx}\right\},$$

$$\left\{O_{10}\right\}=\left[\Sigma_{yz}\right]\left\{\Delta_{zx}\right\},\left\{O_{11}\right\}=\left[\Sigma_{xz}\right]\left\{\Delta_{zy}\right\}\ ,\left\{O_{12}\right\}=\left[\Sigma_{yz}\right]\left\{\Delta_{zy}\right\},$$

$$\left\{O_{13}\right\}=\left[\gamma_{xx}\right]\left\{\Delta_{x}\right\},\left\{O_{14}\right\}=\left[\gamma_{xy}\right]\left\{\Delta_{y}\right\}\ ,\left\{O_{15}\right\}=\left[\gamma_{xy}\right]\left\{\Delta_{x}\right\},$$

$$\left\{O_{16}\right\}=\left[\gamma_{yy}\right]\left\{\Delta_{y}\right\}\ ,\left\{O_{17}\right\}=\left[\Omega_{xz}\right]\left\{\pi_z\right\},\left\{O_{18}\right\}=\left[\Omega_{yz}\right]\left\{\pi_z\right\},$$

$$\left\{O_{19}\right\}=\left[\Sigma_{zx}\right]\left\{\Delta_{xx}\right\},\left\{O_{20}\right\}=\left[\Sigma_{zy}\right]\left\{\Delta_{xy}\right\}\ ,\left\{O_{21}\right\}=\left[\Sigma_{zz}\right]\left\{\Delta_{zx}\right\},$$

$$\left\{O_{22}\right\}=\left[\Sigma_{zx}\right]\left\{\Delta_{yx}\right\},\left\{O_{23}\right\}=\left[\Sigma_{zy}\right]\left\{\Delta_{yy}\right\}\ ,\left\{O_{24}\right\}=\left[\Sigma_{zz}\right]\left\{\Delta_{zy}\right\},$$

$$\left\{O_{25}\right\}=\left[\gamma_{zx}\right]\left\{\Delta_{x}\right\},\left\{O_{26}\right\}=\left[\gamma_{zy}\right]\left\{\Delta_{y}\right\}\ ,\left\{O_{27}\right\}=\left[\Omega_{zz}\right]\left\{\pi_z\right\},$$

where

$$\{O_1\}=\{R_1,R_2,R_3,R_4\},\ \{O_2\}=\{R_5,R_6,R_7,R_8\},\ \{O_3\}=\{R_9,R_{10},R_{11},R_{12}\},$$

$$\{O_4\}=\{R_{13},R_{14},R_{15},R_{16}\},\ \{O_5\}=\{S_1,S_2,S_3,S_4\},\ \{O_6\}=\{S_5,S_6,S_7,S_8\},$$

$$\{O_7\}=\{S_9,S_{10},S_{11},S_{12}\},\ \{O_8\}=\{S_{13},S_{14},S_{15},S_{16}\},\ \{O_9\}=\{R_{17},R_{18},R_{19},R_{20}\},$$

$$\{O_{10}\}=\{S_{17},S_{18},S_{19},S_{20}\},\ \{O_{11}\}=\{R_{21},R_{22},R_{23},R_{24}\},\ \{O_{12}\}=\{S_{21},S_{22},S_{23},S_{24}\},$$

$$\{O_{13}\}=\{R_{30},R_{31},R_{32}\},\ \{O_{14}\}=\{R_{33},R_{34},R_{35}\},\ \{O_{15}\}=\{S_{30},S_{31},S_{32}\},$$

$$\{O_{16}\}=\{S_{33},S_{34},S_{35}\},\ \{O_{17}\}=\{R_{25},R_{26},R_{27}\},\ \{O_{18}\}=\{S_{25},S_{26},S_{27}\},$$

$$\{O_{19}\}=\{U_1,U_2,U_3,U_4\},\ \{O_{20}\}=\{U_5,U_6,U_7,U_8\},\ \{O_{21}\}=\{W_1,W_2,W_3,W_4\},$$

$$\{O_{22}\}=\{U_9,U_{10},U_{11},U_{12}\},\ \{O_{23}\}=\{U_{13},U_{14},U_{15},U_{16}\},\ \{O_{24}\}=\{W_5,W_6,W_7,W_8\},$$

$$\{O_{25}\}=\{V_1,V_2,V_3\},\ \{O_{26}\}=\{V_4,V_5,V_6\},\ \{O_{27}\}=\{W_9,W_{10},W_{11}\},$$

$$\{\Delta_{ij}\}=\left\{u_{i,j}\varphi_{i,j}\xi_{i,j}\phi_{i,j}\right\}^T,(i,j=x,y)\ \ \{\Delta_{zi}\}=\left\{\varphi_i 2\xi_i 3\phi_i\right\}^T,(i=x,y),$$

$$\{\pi_i\}=\left\{\varphi_i 2\xi_i\right\}^T,(i=x,y),\ \{\Delta_i\}=\left\{w_{,i}\ \varphi_{z,i}\ \xi_{z\ i}\right\}^T\ \ (i=,x\ \ y),$$

$$\left[\Sigma_{ij}\right]=\begin{bmatrix} N_{ij} & M_{ij} & M_{ij}^* & P_{ij} \\ M_{ij} & M_{ij}^* & P_{ij} & P_{ij}^* \\ M_{ij}^* & P_{ij} & P_{ij}^* & R_{ij} \\ P_{ij} & P_{ij}^* & R_{ij} & R_{ij}^* \end{bmatrix},(i=x,y,z;j=x,y),$$

$$\left[\Sigma_{iz}\right]=\begin{bmatrix} N_{iz} & M_{iz} & M_{iz}^* \\ M_{iz} & M_{iz}^* & P_{iz} \\ M_{iz}^* & P_{iz} & P_{iz}^* \\ P_{iz} & P_{iz}^* & R_{iz} \end{bmatrix},(i=x,y,z),$$

$$\left[\gamma_{ij}\right]=\begin{bmatrix} N_{ij} & M_{ij} & M_{ij}^* \\ M_{ij} & M_{ij}^* & P_{ij} \\ M_{ij}^* & P_{ij} & P_{ij}^* \end{bmatrix},(i=x,y,z;j=x,y),$$

$$\left[\Omega_{iz}\right]=\begin{bmatrix} N_{iz} & M_{iz} \\ M_{iz} & M_{iz}^* \\ M_{iz}^* & P_{iz} \end{bmatrix},(i=x,y,z)\cdot$$

Here, N_{ij}, M_{ij} and M_{jj}^*, P_{ij}, P_{ij}^*, R_{ij} and R_{ij}^* are the stress resultants associated with arbitrary periodic stresses and are defined as follows:

$$\left(N_{ij},M_{ij},M_{ij}^*,P_{ij},P_{ij}^*,R_{ij},R_{ij}^*\right)=\int\sigma_{ij}\left(1,z,z^2,z^3,z^4,z^5,z^6\right)dz,(i,j=x,y,z),$$

where the higher-order resultants mean high-order moments and shear forces. It should be noted that the high-order resultants are purely mathematical terms and cannot be prescribed on the physical boundaries. The quantities f_x,f_y,f_z, m_x, m_y, m_z, n_x, n_y, n_z, q_x, and q_y are the loads consisting of lateral loads at the top and bottom face of the plate and the body force, and they are given below. The superscripts + and – mean that the stresses are calculated at the top and bottom faces of plate.

$$f_x=\int_{-h/2}^{h/2}\left(\overline{X_x}+\Delta X_x\right)dz+\sigma_{zx}^+-\sigma_{zx}^-,$$

$$f_y=\int_{-h/2}^{h/2}\left(\overline{X_y}+\Delta X_y\right)dz+\sigma_{zy}^+-\sigma_{zy}^-,$$

$$f_z = \int_{-h/2}^{h/2} \left(\bar{X}_z + \Delta X_z\right) dz + \left(\sigma_{zx}^{+} - \sigma_{zx}^{-}\right)\left(w_{,x} + z\varphi_{z,x} + z^2\xi_{z,x}\right)$$

$$+\left(w_{,y} + z\varphi_{z,y} + z^2\xi_{z,y}\right)\left(\sigma_{zy}^{+} - \sigma_{zy}^{-}\right) + \sigma_{zz}^{+} - \sigma_{zz}^{-},$$

$$m_x = \int_{-h/2}^{h/2} \left(\bar{X}_x + \Delta X_x\right) z dz + h\left(\sigma_{zx}^{+} - \sigma_{zx}^{-}\right)/2,$$

$$m_{\mathrm{y}} = \int_{-h/2}^{h/2} \left(\bar{X}_{\mathrm{y}} + \Delta X_{\mathrm{y}}\right) z \mathrm{d}z + h\left(\sigma_{\mathrm{zy}}^{+} - \sigma_{\mathrm{zy}}^{-}\right)/2,$$

$$m_z = \int_{-h/2}^{h/2} \left(\bar{X}_Z + \Delta X_Z\right) z dz + \left(\sigma_{zx}^{+} + \sigma_{zx}^{-}\right)\left(hw_{,x} + z^3\xi_{z,x}/8\right) + \left(h^2/4\right)\varphi_{z,x}\left(\sigma_{zx}^{+} - \sigma_{zx}^{-}\right)$$

$$+\left(hw_{,y} + z^3\xi_{z,y}/8\right)\left(\sigma_{zy}^{+} + \sigma_{zy}^{-}\right) + \left(h^2/4\right)\varphi_{z,y}\left(\sigma_{zy}^{+} - \sigma_{zy}^{-}\right) + z\left(\sigma_{zz}^{+} - \sigma_{zz}^{-}\right)/2,$$

$$n_x = \int_{-h/2}^{h/2} \left(\bar{X}_x + \Delta X_x\right) z^2 dz + h^2\left(\sigma_{zx}^{+} - \sigma_{zx}^{-}\right)/4,$$

$$n_y = \int_{-h/2}^{h/2} \left(\bar{X}_y + \Delta X_y\right) z^2 dz + h^2\left(\sigma_{zy}^{+} - \sigma_{zy}^{-}\right)/4,$$

$$n_z = \int_{-h/2}^{h/2} \left(\bar{X}_Z + \Delta X_Z\right) z^2 dz + \left(\sigma_{zx}^{+} + \sigma_{zx}^{-}\right)\left(h^2 w_{,x}/4 + z^4\xi_{z,x}/16\right) + \left(h^3/8\right)\varphi_{z,x}\left(\sigma_{zx}^{+} - \sigma_{zx}^{-}\right) +$$

$$\left(h^2 w_{,y}/4 + z^4\xi_{z,y}/16\right)\left(\sigma_{zy}^{+} + \sigma_{zy}^{-}\right) + \left(h^3/8\right)\varphi_{z,y}\left(\sigma_{zy}^{+} + \sigma_{zy}^{-}\right) + z^2\left(\sigma_{zz}^{+} - \sigma_{zz}^{-}\right)/4,$$

$$q_x = \int_{-h/2}^{h/2} \left(\bar{X}_x + \Delta X_x\right) z^3 dz + h^3\left(\sigma_{zx}^{+} - \sigma_{zx}^{-}\right)/8,$$

$$q_y = \int_{-h/2}^{h/2} \left(\bar{X}_y + \Delta X_y\right) z^3 dz + h^3\left(\sigma_{zy}^{+} - \sigma_{zy}^{-}\right)/8.$$

The inertia related terms are defined as

$$\left(I_1, I_3, I_5, I_7\right) = \int \rho\left(1, z^2, z^4, z^6\right) dz.$$

REFERENCES

1. V. V. Bolotin, The Dynamic Stability of Elastic Systems, Holden-Day, San Francisco (1964).
2. A. Vijayaraghavan and R. M. Evan-Iwanowski, “Parametric instability of circular cylindrical shells,” J. Appl. Mech., **34**, 985-990 (1967).
3. S. Mohamad, Q. Rani, W. Sullivan, and W. Wang, “Recent research advances on the dynamic analysis of composite shells: 2000-2009,” Composite Structures, **93**, 14-31 (2010).
4. J. Fazilati and H. R. Ovesy, “Dynamic instability analysis of composite laminated thin-walled structures using two versions of FSM,” Composite Structures, **92**, 2060-2065 (2010).

5. H. R. Ovesy and J. Fazilati, "Parametric instability analysis of laminated composite curved shells subjected to non-uniform in-plane load," Composite Structures **108**, 449-455 (2014).
6. J. Y. Kao, C. S. Chen, and W. R. Chen, "Parametric vibration response of foam-filled sandwich plates under periodic loads," Mech. Compos. Mater., **48**, 525-538 (2012).
7. W. R. Chen, C. S. Chen, and J. H. Shyu, "Stability of parametric vibrations of laminated composite plates," Applied Mathematics and Computation, **223**, 127-138 (2013).
8. M. Darabi and R. Ganesan, "Nonlinear dynamic instability analysis of laminated composite thin plates subjected to periodic in-plane loads," Nonlinear Dynamics, **91**, 187-215 (2018).
9. R. Sahoo and B. N. Singh, "Assessment of dynamic instability of laminated composite-sandwich plates," Aerospace Science and Technology, **81**, 41-52 (2018).
10. M. Rasool and M. K. Singha, "Stability behavior of variable stiffness composite panels under periodic in-plane shear and compression," Composites, Part B: Engineering, **172**, 472-484 (2019).
11. J. Mohanty, S. K. Sahu, and P. K. Parhi, "Parametric instability of delaminated composite plates subjected to periodic in-plane loading," Journal of Vibration and Control, **21**, 419-434 (2015).
12. S. Y. Lee, "Finite element dynamic stability analysis of laminated composite skew plates containing cutouts based on HSDT," Composites Science and Technology, **70**, 1249-1257 (2010).
13. A. Sankar, S. Natarajan, and M. Ganapathi, "Dynamic instability analysis of sandwich plates with CNT reinforced facesheets," Composite Structures, **146**, 187-200 (2016).
14. L. S. Ramachandra and S. K. Panda, "Dynamic instability of composite plates subjected to non-uniform in-plane loads," Journal of Sound and Vibration, **331**, 53-65 (2012).
15. M. H. Noh and S.Y. Lee, "Dynamic instability of delaminated composite skew plates subjected to combined static and dynamic loads based on HSDT," Composites, Part B: Engineering, **58**, 113-121 (2014).
16. R. A. Kumar and S. K. Panda, "Parametric resonance of composite skew plate under non-uniform in-plane loading," Structural Engineering and Mechanics, **55**, 435-459 (2015).
17. B. Adhikari and B. N. Singh, "Parametric instability analysis of laminated composite plate subject to various types of non-uniform harmonic in-plane edge load," Applied Mathematics and Computation, **373**, 125026 (2020).
18. K. H. Lo, R. M. Christensen, and E. M. Wu, "A high-order theory of plate deformation, part 2: Laminated plates," Transactions ASME. Journal of Applied Mechanics, **44**, 669-676 (1977).
19. E. J. Brunell and S. R. Robertson, "Vibrations of an initially stressed thick plate," Journal of Sound and Vibration, **45**, 405-416 (1976).
20. E. Reissner, "The effect of transverse shear deformation on the bending of elastic plates," Transactions ASME. Journal of Applied Mechanics, **12**(2), 69-77 (1945).
21. R. D. Mindlin, "Influence of rotary inertia and shear on flexural motions of isotropic elastic plates," Transactions ASME, Journal of Applied Mechanics, **18**(1), 31-38, 1951.
22. F. Essenburge, "On the significance of the inclusion of the effect of transverse normal strain in problem involving beams with surface constrains," Transactions ASME, Journal of Applied Mechanics, **42**, 127-132 (1975).
23. B. N. Pandya and T. Kant, "Finite element stress analysis of laminated composite plates using higher order displacement model," Composites Science and Technology, **32**, 137-155 (1988).
24. M. Levinson, "An accurate simple theory of the statics and dynamics of elastic plates," Mechanics Research Communications, **7**(6), 343-350 (1980).
25. J. N. Reddy, "A simple high-order theory for laminated composite plates," Transactions ASME, Journal of Applied Mechanics, **51**(4), 745-752 (1984).
26. C. S. Chen, C. Y. Hsu, and G. J. Tzou, "Vibration and stability of functionally graded plates based on a high-order deformation theory," Journal of Reinforced Plastics and Composites, **28**, 1215-1234 (2009).
27. J. M. Whitney and N. J. Pagano, "Shear deformation in heterogeneous anisotropic plates," Transactions ASME, Journal of Applied Mechanics, **37**(4), 1031-1036 (1970).
28. T. Kant and K. Swaminathan, "Analytical solutions for free vibration of laminated composite and sandwich plates based on a high-order refined theory," Composite Structures, **53**, 73-85 (2001).

29. S. Wang and D. J. Dawe, “Dynamic instability of composite laminated rectangular plates and prismatic plate structures,” Computer Methods in Applied Mechanics and Engineering, **191**, 1791-1826 (2002).
30. W. R. Chen, C. S. Chen, and J. H. Shyu “Stability of parametric vibrations of laminated composite plates” Applied Mathematics and Computation, **223**, 127-138 (2013).